ORIGINAL ARTICLE

Expression profiling analysis: Uncoupling protein 2 deficiency improves hepatic glucose, lipid profiles and insulin sensitivity in high-fat diet-fed mice by modulating expression of genes in peroxisome proliferator-activated receptor signaling pathway

Mei-Cen Zhou[1], Ping Yu[2], Qi Sun[1], Yu-Xiu Li[1]*

[1]Department of Endocrinology, Key Laboratory of Endocrinology, Ministry of Health, Peking Union Medical College Hospital, Beijing and [2]Department of Pharmacy, the Third People's Hospital, Qinhuangdao, China

ABSTRACT

Aims/Introduction: Uncoupling protein 2 (UCP2), which was an important mitochondrial inner membrane protein associated with glucose and lipid metabolism, widely expresses in all kinds of tissues including hepatocytes. The present study aimed to explore the impact of UCP2 deficiency on glucose and lipid metabolism, insulin sensitivity and its effect on the liver-associated signaling pathway by expression profiling analysis.

Materials and Methods: Four-week-old male UCP2–/– mice and UCP2+/+ mice were randomly assigned to four groups: UCP2–/– on a high-fat diet, UCP2–/– on a normal chow diet, UCP2+/+ on a high-fat diet and UCP2+/+ on a normal chow diet. The differentially expressed genes in the four groups on the 16th week were identified by Affymetrix gene array.

Results: The results of intraperitoneal glucose tolerance test and insulin tolerance showed that blood glucose and β-cell function were improved in the UCP2–/– group on high-fat diet. Enhanced insulin sensitivity was observed in the UCP2–/– group. The differentially expressed genes were mapped to 23 pathways ($P < 0.05$). We concentrated on the 'peroxisome proliferator-activated receptor (PPAR) signaling pathway' ($P = 3.19 \times 10^{-11}$), because it is closely associated with the regulation of glucose and lipid profiles. In the PPAR signaling pathway, seven genes (*PPARγ*, *Dbi*, *Acsl3*, *Lpl*, *Me1*, *Scd1*, *Fads2*) in the UCP2–/– mice were significantly upregulated.

Conclusions: The present study used gene arrays to show that activity of the PPAR signaling pathway involved in the improvement of glucose and lipid metabolism in the liver of UCP2-deficient mice on a long-term high-fat diet. The upregulation of genes in the PPAR signaling pathway could explain our finding that UCP2 deficiency ameliorated insulin sensitivity. The manipulation of UCP2 protein expression could represent a new strategy for the prevention and treatment of diabetes.

INTRODUCTION

Islet β-cell dysfunction and insulin resistance are two major pathophysiological mechanisms in type 2 diabetes mellitus[1,2]. Excessive fatty acid intake could cause a decline in insulin

sensitivity, and long-term excessive fatty acid intake could result in β-cell dysfunction and a relative lack of insulin secretion, leading to the development of type 2 diabetes[3].

Uncoupling protein 2 (UCP2), which is a member of the mitochondrial inner membrane carrier family, is expressed widely in a number of tissues and cell types[4], including islet β-cells and hepatocytes[5,6]. The effects of UCP2 on proton leakage and the decline in adenosine triphosphate (ATP) synthesis in islet β-cells is involved in glucose-stimulated insulin secretion. Increased levels of glucose induce an increase in the ATP/adenosine diphosphate ratio in the mitochondria, which inhibits ATP-sensitive potassium (K_{ATP}) channels, leading to plasma membrane depolarization and an increase in insulin secretion[7–9], the expression of UCP2 could decrease the ATP synthesis and result in the decline of insulin secretion. The effects of UCP2 on proton leakage and the decline in ATP synthesis in β-cells show that this protein is a negative regulator of insulin secretion[5–7].

The liver is of great importance in the regulation of glucose and lipid metabolism, including insulin sensitivity. Though UCP2 level is very low in hepatocytes in the normal state, it significantly increases in a high-fat diet-fed state[10]. Many studies have shown the effect of UCP2 on islet β-cells insulin secretion[5,10–12]; however, more studies are required to further investigate the influence of UCP2 deficiency on the changes of the glucose and lipid metabolism-associated signaling pathways, and the expression of the related genes in the liver. The present study aimed to assess the impact of UCP2 deficiency on the liver-associated glucose and lipid metabolism, and insulin sensitivity to explore the underlying signaling pathway through expression profiling analysis.

MATERIALS AND METHODS

Animals

The animal care and use committee of the Peking Union Medical College Hospital (Beijing, China, MC-07-6004, 3 May 2013) approved all the procedures. All the operations involving animals were carried out according to the Guide for the Care and Use of Laboratory Animals. Four-week-old male UCP2−/− mice with C57BL/6 backgrounds and the control UCP2+/+ mice with the same C57BL/6 backgrounds (UCP2−/− mice and UCP2+/+ mice were littermates from crossing between ±males and ±female) were obtained from the Institute of Laboratory Animal Science, Chinese Academy of Medical Sciences and Peking Union Medical College (the institute acquired UCP2−/− mice from the Jackson Laboratory in 2011). All mice were housed (5 mice/cage) in an air-conditioned room at 22 ± 2°C under controlled ambient conditions and a 12-h light/12-h dark cycle. After arrival and 1 week of acclimatization, UCP2−/− mice and UCP2+/+ mice were randomly assigned to four groups as follows: UCP2−/− mice on a high-fat diet (n = 10), UCP2−/− mice on a normal chow diet (n = 10), UCP2+/+ mice on a high-fat diet (n = 10) and UCP2+/+ mice on a normal chow diet (n = 10). The high-fat diet contained the following (kcal%): fat (lard) 58%, carbohydrate 25.6%, protein 16.4% and the energy density was 23.4 kJ/g. The normal chow diet contained the following (kcal%): 11.4% fat, 62.8% carbohydrate and 25.8% protein, and the energy density was 12.6 kJ/g. Drinking water and food were supplied *ad libitum* for 16 weeks. Bodyweight and fasting blood glucose (FBG) were measured every 4 weeks. FBG was measured with a Glucometer Elite (Optium Xeed; Abbott, Oxon, UK) using blood from the tail vein.

Laboratory evaluation

At baseline and week 16, the fasting serum insulin concentration was measured using an ELISA kit (EZRMI-13K; Millipore, St. Charles, MO, USA). The serum total cholesterol, triglyceride and free fatty acid concentrations were measured with a Beckman CX4 automatic biochemical analyzer (Beckman Coulter, Inc., Brea, CA, USA; intra-assay CV <3%).

Intraperitoneal glucose tolerance test and insulin tolerance test

At the 16th week, after an overnight fast, mice were intraperitoneally injected with 1.5 g/kg of glucose (time 0). Blood glucose

Table 1 | Oligonucleotide sequences for messenger ribonucleic acid quantitative reverse transcription polymerase chain reaction

Gene symbol	Forward primer (5′–3′)	Reverse primer (5′–3′)
PPARγ	AGACCACTCGCATTCCTTTGAC	GCAGGTTCTACTTTGATCGCACT
Acsl3	AGACCAGGGCTGAGTGGATGAT	CAGACGTGGGACCAAAGAGACTAT
Dbi	GTGGAAAAGGTAGACGAGCTAAAGA	TACAGAGGGAGGAGGAGCAGAG
Lpl	TCATCTCTTCATTGACTCCCTGCTG	TGCTTCTCTTGGCTCTGACCTTGT
Me1	GAGTTGCTCTTGGGGGTGGTG	GGCCTTCTTGCAGGTGTTTATC
Scd1	GTCAAAGAGAAGGGCGGAAAAC	CACCAGAGTGTATCGCAAGAAGG
Fads2	CAGCCTTTGTCCTCGCTACCTC	GGCATGGTGTTGGAAATGTCGG
PPARα	GGCAAAAGGCAAGGAGAAGCA	GGGAAAGAGGTGAGAGAAGAGCG
PPARδ	ACCTCCTGTTCTTGCTGTCTCCC	AACGGGCTGTCTGCTGTGAATC
β-actin	TGTTACCAACTG GGACGACA	GGGGTGTTGAAGGTCT CAAA

Acsl3, acyl-CoA synthetase long-chain family member 3; Dbi, diazepam binding inhibitor; Fads2, fatty acid desaturase 2; Lpl, lipoprotein lipase; Me1, malic enzyme 1; PPARα, peroxisome proliferator-activated receptor alpha; PPARδ, peroxisome proliferator-activated receptor delta; PPARγ, peroxisome proliferator-activated receptor gamma; Scd1, stearoyl-CoA desaturase 1.

Table 2 | Comparison of uncoupling protein 2–/– group and uncoupling protein 2+/+ group at baseline

	UCP2+/+ (n = 10)	UCP2–/– (n = 10)
FBG (mmol/L)	5.05 ± 0.53	4.54 ± 1.24
Fasting insulin (ng/mL)	0.27 ± 0.09	0.29 ± 0.22

There were no significant differences between the groups. FBG, fasting blood glucose; UCP2, uncoupling protein 2.
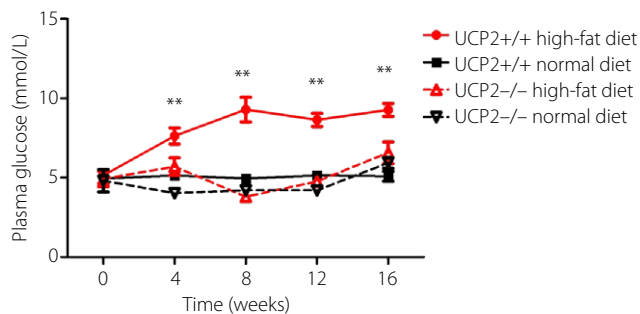

Figure 1 | Fasting blood glucose was measured every 4 weeks and was found to significantly differ in the uncoupling protein 2 (UCP2)–/– group on the high-fat diet compared with the UCP2+/+ group on the high-fat diet. There was no significant difference in fasting blood glucose between the UCP2–/– group on the high-fat diet vs the normal chow diet group. **$P < 0.01$.

levels were assessed at 0, 15, 30, 60 and 120 min for the intraperitoneal glucose tolerance test (IPGTT; n = 10 per group). After 4 days, after 6 h without food, the mice were injected with 0.75 U/kg of insulin, i.p. (time 0). Blood glucose values were assessed before injection, and at 15, 30, 60 and 90 min after injection. The areas under the curves (AUCs) of IPGTT and insulin tolerance test (ITT) were respectively calculated by the trapezoid formula as follows: AUC (IPGTT) = 15 × (VAL0 + VAL15)/ 2 + 15 × (VAL15 + VAL30)/2 + 30 × (VAL30 + VAL60)/ 2 + 60 × (VAL60 + VAL120)/2, AUC (ITT) = 15 × (VAL0 + VAL15)/2 + 15 × (VAL15 + VAL30)/2 + 30 × (VAL30 + VAL 60)/2 + 30 × (VAL60 + VAL90)/2. β-Cell function was estimated as the ratio of incremental insulin ($\triangle I_{30}$) to glucose ($\triangle G_{30}$) responses during the first 30 min of the IPGTT ($\triangle I / \triangle G = I_{30} - I_0 / G_{30} - G_0$; the acute insulin response to glucose [AIRg]), the insulin sensitivity index (Si = $1/G_0 \times I_0$) and the disposition index (AIRg × Si).

Histopathological evaluation

Liver samples were prepared for oil red O staining and were immersion-fixed overnight in 10% formalin (v/v) at 4°C. The tissues were then routinely processed for paraffin embedding, and 5-μm sections mounted on glass slides were processed for hematoxylin–eosin staining (n = 10 per group).

All the histopathological findings were scored by experienced pathologists (n = 10 per group), who were unaware of the genetic backgrounds and diets of the mice. The level of steatosis was scored according to the NASH/NAFLD Clinical Research Network scoring system definitions and scores[13].

Ribonucleic acid preparation and gene array experiments

At the 16th week, liver tissues from the four groups were obtained to carry out the array experiments (n = 3 per group). Total ribonucleic acid (RNA) from the liver tissues was extracted using TRIzol reagent (Invitrogen, Carlsbad, CA, USA) and purified with an RNeasy Mini Kit (Qiagen, Hilden, Germany). The concentration and purity of the total RNA were assessed with an Agilent 2100 Bioanalyzer. Complementary deoxyribonucleic acid was synthesized from the total RNA using a reverse transcriptase synthesis system (Superscript II; Invitrogen). The gene expression profiles in the mouse liver tissues were determined using genome-wide gene expression arrays. Each group contained three biological replicates to obtain a relatively reliable estimate of the mean gene expression. Therefore, a total of 12 gene arrays were analyzed. The samples were processed following Affymetrix recommendations,

Table 3 | Comparison of uncoupling protein 2–/– groups and uncoupling protein 2+/+ groups after 16 weeks

	UCP2+/+ on high fat diet (n = 10)	UCP2–/– on high fat diet (n = 10)	UCP2+/+ on normal diet (n = 10)	UCP2–/– on normal diet (n = 10)
Weight gain	8.55 ± 2.38**	8.57 ± 3.44**	6.23 ± 2.06	7.02 ± 1.93
Liver/bodyweight (100×)	6.42 ± 0.61	6.31 ± 0.46	6.11 ± 0.59	6.18 ± 0.65
FBG (mmol/L)	9.27 ± 1.25**	6.57 ± 2.17	5.09 ± 1.01	5.93 ± 1.04
Fasting insulin (ng/mL)	0.24 ± 0.10	0.41 ± 0.19**	0.27 ± 0.09	0.26 ± 0.08
AIRg	0.09 ± 0.01*	0.11 ± 0.02	0.14 ± 0.03	0.13 ± 0.01
Si	0.32 ± 0.11*	0.45 ± 0.07	0.41 ± 0.08	0.44 ± 0.09
Disposition index	0.03 ± 0.01*	0.05 ± 0.01	0.05 ± 0.02	0.06 ± 0.02

*$P < 0.05$, **$P < 0.01$. AIRg, acute insulin response to glucose; FBG, fasting blood glucose; Si, sensitivity index; UCP2, uncoupling protein 2.
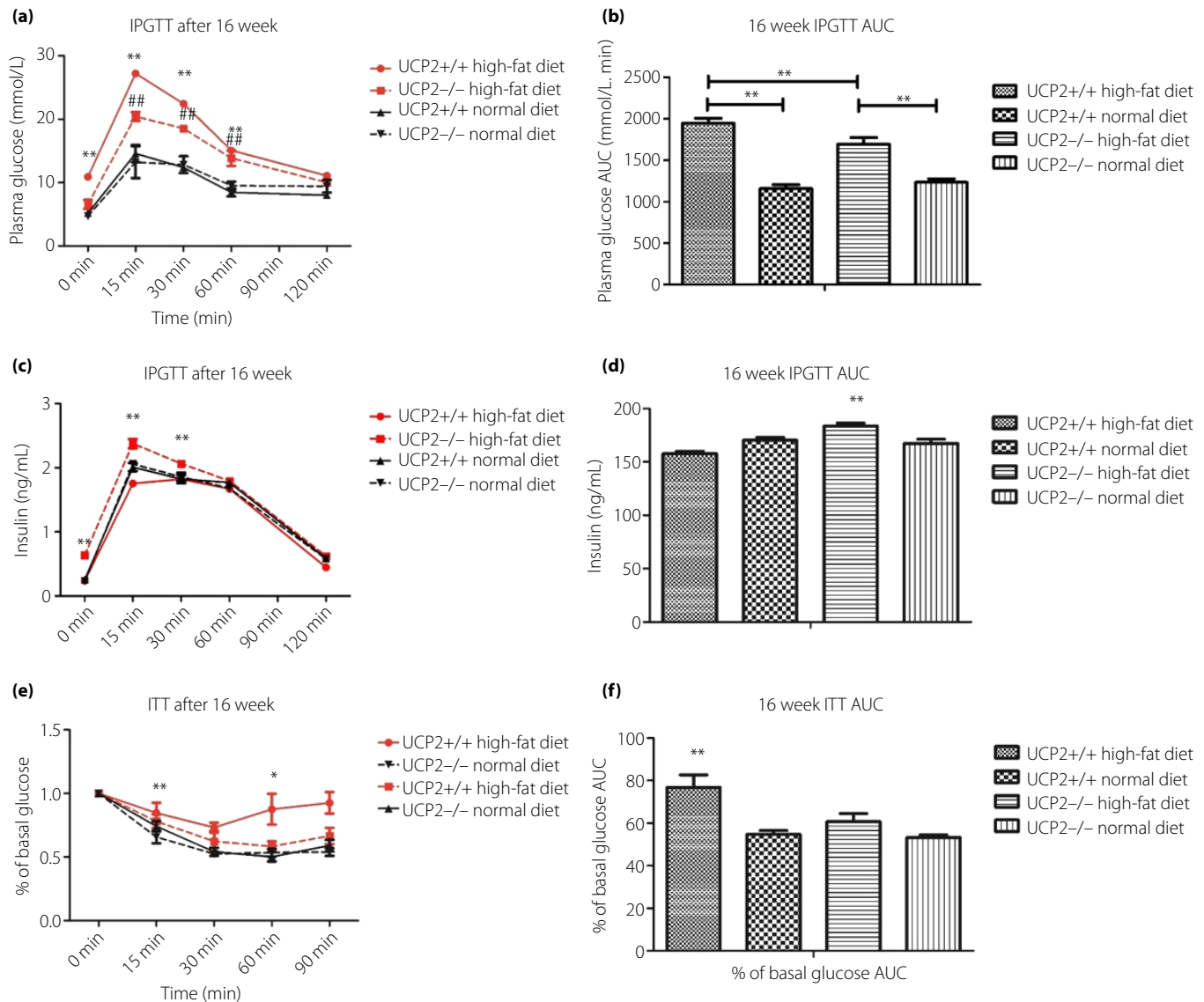
Figure 2 | Two-hour intraperitoneal glucose tolerance test intraperitoneal glucose tolerance test (IPGTT): plasma glucose profiles in response to (a) an exogenous glucose load and (b) area under the curve (AUC), (c) serum insulin profiles in response to an exogenous glucose load and (d) AUC; (e) insulin tolerance test (ITT): plasma glucose profiles in response to exogenously administered insulin and (f) AUC. *$P < 0.05$, **$P < 0.01$, ##$P < 0.01$. UCP2, uncoupling protein 2.

and the complementary deoxyribonucleic acid was hybridized to an Affymetrix Mouse Gene ST 1.0 array (Affymetrix, Santa Clara, CA, USA).

The signals were averaged for the liver tissues from the high-fat diet and normal chow diet groups, and fold changes were calculated based on the average values from each group. The differentially expressed genes between the UCP2−/− groups and UCP2+/+ groups defined as: (the differentially expressed genes between UCP2−/− group on high-fat diet and UCP2−/− group on normal diet) − (the differentially expressed genes between UCP2+/+ group on high-fat diet and UCP2+/+ group on normal diet). Genes were selected as significant using a combined

criterion for true positive expression differences of a fold change >1.5 and a *P*-value <0.05. Cluster analyses were carried out using g-plots R package (O'Reilly media, Sebastopol, CA, USA). To identify the biological significance of the group of genes with changed expression, the subset of genes that met the aforementioned criteria was analyzed using the Gene Ontology (GO) classification system, and the Kyoto Encyclopedia of Genes and Genomes pathway database. Fisher's exact test was used to assess the significance of the GO classification and pathway analysis results, and only GO terms with a *P* < 0.01 were considered enriched. The threshold of significance for the pathway analysis was set to *P* < 0.05.

Quantitative reverse transcription polymerase chain reaction experiment

To validate the array results, seven upregulated genes (listed in Table 1) in the peroxisome proliferator-activated receptor (PPAR) signaling pathway were selected for quantitative reverse transcription polymerase chain reaction (RT–qPCR) analysis of the samples in the four groups ($n = 10$ per group). Furthermore, we investigated the expression of an additional two PPAR isoforms, PPARα and PPARδ, in the four groups ($n = 10$ per group). The RT–qPCR experimental protocol has been previously described[14]. The sequences of the primers used are listed in Table 1.

Statistical analysis

SPSS 17.0 software (SPSS, Chicago, IL, USA) was used for statistical analysis. The data were normally distributed and were expressed as the mean ± standard deviation. Statistical analyses were carried out with ANOVA followed by Student's t-test. The random variance model t-test was applied to filter the differentially expressed genes in the control and experimental groups. A P-value <0.05 showed statistical significance.

RESULTS

UCP2 deficiency improved blood glucose by simultaneously regulating islet β-cell function and insulin sensitivity

At baseline, there were no significant differences in FBG or fasting serum insulin between the UCP2–/– and UCP2+/+ mice (Table 2). At 4, 8, 12 and 16 weeks, the FBG in the UCP2–/– group was lower than that in the UCP2+/+ group on the high-fat diet, and there was no significant difference in FBG between the UCP2–/– group on the high-fat diet vs the normal chow diet groups (Figure 1). In the 16th week of high-fat diet intake, the serum fasting insulin concentration in the UCP2–/– group on the high-fat diet was higher (Table 3).

On the 16th week of the high-fat diet treatment, a 2-h IPGTT was carried out to investigate the response to an
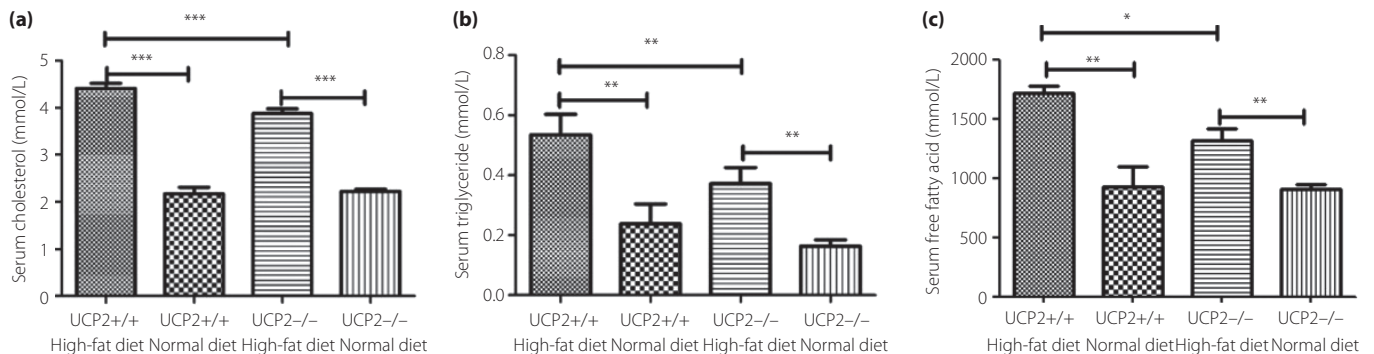

Figure 3 | In the 16th week, the following serum lipid concentrations were measured among the groups: (a) serum total cholesterol; (b) serum triglycerides; and (c) serum free fatty acid. ***$P < 0.001$, **$P < 0.01$, *$P < 0.05$. UCP2, uncoupling protein 2.
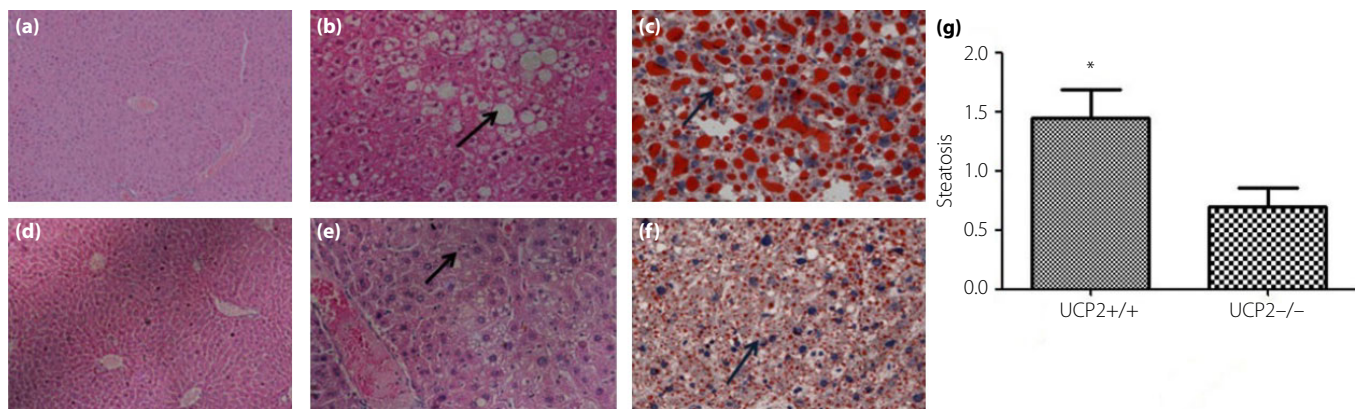

Figure 4 | (a–e) Hematoxylin–eosin staining staining at the 16 weeks. (a) Uncoupling protein 2 (UCP2)+/+ group in normal diet (black arrow, steatosis; magnification: ×10). (b) UCP2+/+ group on the high-fat diet (magnification: ×20). (c) UCP2–/– group in normal diet (magnification: ×10). (e) UCP2–/– group on the high-fat diet (magnification: ×20). (c, f) Oil red O staining at 16 weeks (blue arrow, red lipid droplet; magnification: ×10). (c) UCP2+/+ group on the high-fat diet (magnification: ×40). (f) UCP2–/– group on the high-fat diet (magnification: ×40). (g) Histopathological evaluation of steatosis in the UCP2+/+ group and UCP2–/– group on the high-fat diet. *$P < 0.05$.
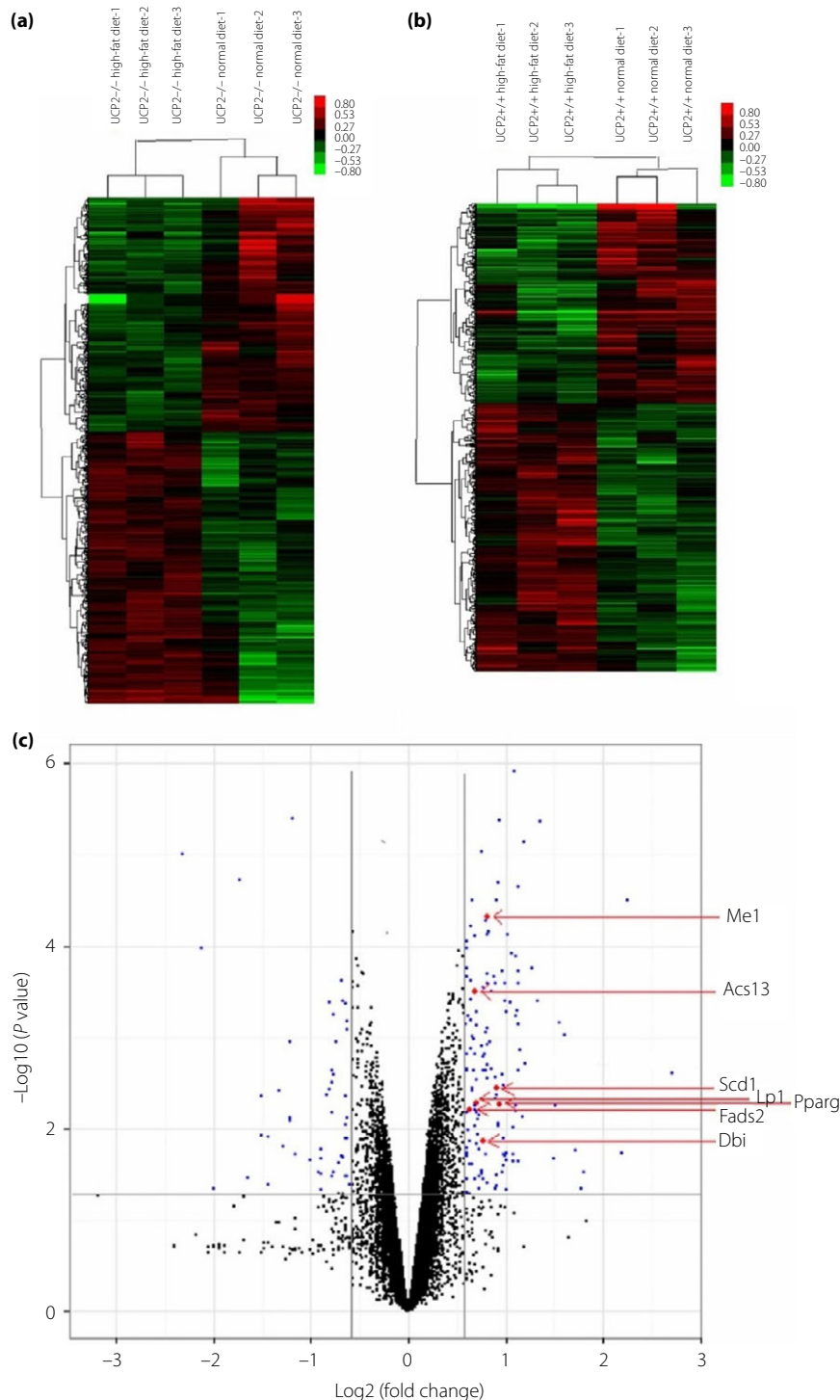
Figure 5 | Gene array data analysis comparing the gene expression of the uncoupling protein 2 (UCP2)–/– groups with that of the UCP2+/+ groups. (a) Heat map diagram: the differential expression of hepatic messenger ribonucleic acids between the UCP2–/– group on high-fat diet and the UCP2–/– group on the normal diet. The tree was based on the log2 transformation of the normalized probe signal intensities using hierarchical clustering. The hierarchical clustering was based on the differentially expressed messenger ribonucleic acids. (b) Heat map diagram: the differential expression of hepatic messenger ribonucleic acids between the UCP2+/+ group on the high-fat diet and the UCP2+/+ group on the normal diet. (c) Volcano plot: this graph shows the log2 of the fold change in the expression of each gene between the UCP2–/– groups and the UCP2+/+ groups, and the *P*-values obtained from the *t*-test. The blue plots show that the threshold for the fold change in gene expression was >1.5, and the *P*-value was <0.05. The red plots show the upregulated genes in the peroxisome proliferator-activated receptor signaling pathway.

exogenous glucose load, and a 90-min ITT was carried out to explore sensitivity to exogenously administered insulin. The blood glucose of the UCP2+/+ group and the UCP2–/– group on the high-fat diet were significantly higher at 15, 30 and 60 min compared with these groups on the normal diet after intraperitoneal glucose administration (Figure 2a), the AUC in the high-fat diet groups was also higher than that in the normal diet groups (Figure 2b). In the high-fat diet groups, the blood glucose levels of the UCP2+/+ group were significantly higher at 0, 15, 30 and 60 min compared with the UCP2–/– group after intraperitoneal glucose administration (Figure 2a), and the AUC of the UCP2+/+ group was significantly higher than that of the UCP2–/– group (Figure 2b). The serum insulin levels of the UCP2–/– group on the high-fat diet were significantly higher at 0, 15 and 30 min compared with the UCP2+/+ group on the high-fat diet after intraperitoneal glucose administration, there was no significant difference in the serum insulin levels between the UCP2+/+ group on the high-fat diet and the normal chow diet groups (Figure 2c), and the AUC of the UCP2–/– group on the high-fat diet was significantly higher than that of other three groups (Figure 2d). Furthermore, the ITT showed that the blood glucose levels of the UCP2+/+ group on the high-fat group were significantly higher at 15 and 60 min (Figure 2e) compared with the other three groups, the AUC in the UCP2+/+ group on the high-fat group was higher than the other three groups (Figure 2f). The β-cell function and insulin sensitivity index including AIRg, Si and disposition index in these four groups are listed in Table 3. The AIRg, Si and disposition index were higher in the UCP2–/– group compared with that in UCP2+/+ group after 16 weeks on the high-fat diet.

UCP2 deficiency improved lipid profiles

On the 16th week of the high-fat diet treatment, the serum total cholesterol, triglyceride and free fatty acid concentrations were significantly higher in the high-fat diet groups than that in the normal chow diet groups. The serum total cholesterol, triglyceride and free fatty acid concentrations were significantly

lower in the UCP2–/– group on the high-fat diet than in the UCP2+/+ group on the high-fat diet (Figure 3).

In the 16th week of the high-fat diet treatment, the liver hematoxylin–eosin staining and oil red O staining showed that the hepatocytes in the UCP2+/+ group (Figure 4b,c) and UCP2–/– group (Figure 4e,f) had mild to moderate steatosis. Hepatocyte steatosis scores were significantly higher in the UCP2+/+ group on the high-fat diet than in the UCP2–/– group on the high-fat diet (Figure 4g).

UCP2 deficiency regulated gene expression in response to a high-fat diet

The differentially expressed genes between the UCP2–/– group and UCP2+/+ group were identified (the differentially expressed genes between the UCP2–/– groups and UCP2+/+ groups defined as: [the differentially expressed genes between UCP2–/– group on high-fat diet and UCP2–/– group on normal diet] – [the differentially expressed genes between UCP2+/+ group on the high-fat diet and UCP2+/+ group on the normal diet]). There were 194 differentially expressed genes identified in the liver tissues. Among them, 144 genes (74.2%) were expressed at increased levels, and 50 (25.8%) were expressed at decreased levels. Hierarchical clustering based on similarities in gene expression using all of the differentially expressed genes highlighted the differences in the transcriptional profiles between the UCP2–/– groups and UCP2+/+ groups (Figure 5a–c). A total of 79 GO categories were identified for the differentially expressed genes in the UCP2–/– group (Table 4; list of top 10 GO categories) in addition to 23 Kyoto Encyclopedia of Genes and Genomes pathways ($P < 0.05$, Table 5).

The top enriched Kyoto Encyclopedia of Genes and Genomes pathway was identified to be 'Drug metabolism-cytochrome P450' ($P = 6.92 \times 10^{-16}$). The second and third most enriched pathways were 'Chemical carcinogenesis' ($P = 2.21 \times 10^{-12}$) and 'Metabolism of xenobiotics by cytochrome P450' ($P = 2.44 \times 10^{-12}$), respectively. The fourth most abundant pathway was the 'PPAR signaling pathway'

Table 4 | Gene ontology groups of differentially upregulated genes in uncoupling protein 2–/– group

GO ID	GO name	Enrichment	P-value	FDR
GO:0055114	Oxidation-reduction process	10.87	8.48×10^{-12}	3.25×10^{-09}
GO:0008152	Metabolic process	8.72	1.28×10^{-11}	3.25×10^{-09}
GO:0006633	Fatty acid biosynthetic process	50.13	4.49×10^{-10}	7.61×10^{-08}
GO:0006629	Lipid metabolic process	12.91	4.73×10^{-09}	6.01×10^{-07}
GO:0006810	Transport	5.04	7.48×10^{-08}	7.60×10^{-06}
GO:0006631	Fatty acid metabolic process	20.71	2.07×10^{-06}	0.000175
GO:0043123	Positive regulation of I-kappa B kinase/NF-kappa B cascade	22.85	1.18×10^{-05}	0.000858
GO:0000038	Very-long-chain fatty acid metabolic process	89.97	1.94×10^{-05}	0.001231
GO:0001676	Long-chain fatty acid metabolic process	68.55	4.57×10^{-05}	0.002185
GO:0006082	Organic acid metabolic process	319.89	5.16×10^{-05}	0.002185

Top 10 gene ontology (GO) categories, $P < 0.01$. FDR, false discovery rate.

Table 5 | Kyoto Encyclopedia of Genes and Genomes pathways of differentially upregulated genes in uncoupling protein 2–/– group

KEGG ID	Pathway name	Gene symbol	Enrichment	*P*-value	FDR
00982	Drug metabolism-cytochrome P450	*Mgst3, Cyp2c55, Cyp2c38, Fmo1, Cyp2a4, Cyp2b9, Gsta3, Gsta4, Gsta1, Gsta2, Fmo2*	54.41	6.92×10^{-16}	6.71×10^{-14}
05204	Chemical carcinogenesis	*Cyp2b9, Cyp2c38, Cyp2a4, Gsta3, Gsta4, Gsta1, Gsta2, Mgst3, Cyp2c55*	45.45	2.21×10^{-12}	7.89×10^{-11}
00980	Metabolism of xenobiotics by cytochrome P450	*Mgst3, Cyp2c55, Gsta4, Cyp2a4, Cyp2b9, Gsta3, Gsta2, Cyp2c38, Gsta1*	44.98	2.44×10^{-12}	7.89×10^{-11}
03320	PPAR signaling pathway	*PPARγ, Dbi, Acsl3, Lpl, Me1, Scd1, Fads2*	47.39	3.19×10^{-11}	7.73×10^{-10}
01100	Metabolic pathways	*Cyp2c38, Ces1e, Cyp2b9, Acsl3, Acot3, Cyp2a4, Gclc, Cyp2c55, Acot4, Me1, Acaca, B3galt1, Akrld1, Tkt, Ces1d, Cyp2r1*	6.57	4.04×10^{-09}	7.85×10^{-08}
01040	Biosynthesis of unsaturated fatty acids	*Acot3, Acot4, Scd1, Fads2, Fads1*	95.97	7.43×10^{-09}	1.07×10^{-07}
00480	Glutathione metabolism	*Mgst3, Gclc, Gsta3, Gsta2, Gsta1, Gsta4*	52.35	7.71×10^{-09}	1.07×10^{-07}
00983	Drug metabolism – other enzymes	*Ces1d, Cyp2a4, Ces1e, Ces2e*	31.46	3.42×10^{-05}	0.00041
00830	Retinol metabolism	*Cyp2c55, Cyp2a4, Cyp2c38, Cyp2b9*	22.06	0.000139	0.00142
04640	Hematopoietic cell lineage	*Il1a, Mme, Cd24a*	21.81	0.000146	0.00142
00061	Fatty acid biosynthesis	*Fasn, Acaca*	159.94	0.000257	0.00227
04614	Renin-angiotensin system	*Mme, Enpep*	45.70	0.003526	0.02850
00062	Fatty acid elongation	*Acot3, Acot4*	39.99	0.004615	0.03221
00590	Arachidonic acid metabolism	*Cyp2c38, Cyp2c55, Cyp2b9*	14.69	0.004650	0.03221
04710	Circadian rhythm	*Rorc, Cry1*	30.96	0.007701	0.04980
04910	Insulin signaling pathway	*Socs2, Fasn, Acaca*	10.21	0.013101	0.07479
05166	HTLV-I infection	*Nfyb, Fzd4, Pttf1, Vac14*	6.62	0.013108	0.07479
00620	Pyruvate metabolism	*Me1, Acaca*	22.85	0.014048	0.07570
02010	ABC transporters	*Abcd2, Abcg2*	20.86	0.016795	0.08574
00591	Linoleic acid metabolism	*Cyp2c38, Cyp2c55*	19.19	0.019771	0.09588
05152	Tuberculosis	*Il1a, Nfyb, Plk3*	8.04	0.025432	0.11747
04920	Adipocytokine signaling pathway	*Acsl3*	13.52	0.038981	0.17187
04260	Cardiac muscle contraction	*Slc9a6, Tpm2*	12.15	0.047810	0.20164

Fold change >1.5, $P < 0.05$. FDR, false discovery rate; HTLV-I, human T-cell leukemia virus 1; KEGG, Kyoto Encyclopedia of Genes and Genomes; PPAR, peroxisome proliferator-activated receptor.

($P = 3.19 \times 10^{-11}$). The other pathways are listed in Table 5. We concentrated on the 'PPAR signaling pathway,' because it is closely associated with the regulation of glucose and lipid profiles. In this pathway, seven genes were significantly upregulated according to the gene array, including *PPARγ* (peroxisome proliferator-activated receptor gamma), *Dbi* (diazepam binding inhibitor), *Acsl3* (acyl-CoA synthetase long-chain family member 3), *Lpl* (lipoprotein lipase), *Me1* (malic enzyme 1), *Scd1* (stearoyl-CoA desaturase 1) and *Fads2* (fatty acid desaturase 2). The expression ratios were presented as the $\log_2$ (fold change; Figure 5b).

Hepatic gene expression in the PPAR signaling pathway for validation of array analysis

We used RT–qPCR to verify the results of the gene array. Seven genes (*PPARγ, Dbi, Acsl3, Lpl, Me1, Scd1* and *Fads2*) in the PPAR signaling pathway were upregulated according to the RT–qPCR assay, which was consistent with the gene array. UCP2 messenger RNA (mRNA) levels were significantly higher in UCP2+/+ group on the high-fat diet than that on the normal diet (fold change 2.1 ± 0.11, $P < 0.01$). Furthermore, we investigated the expression of other PPAR isoforms, PPARα and PPATδ, to explain the regulation of the PPAR pathway in

Table 6 | Fold change of differential gene expression in liver as measured by gene array and quantitative reverse transcription polymerase chain reaction at the 16th week

	Gene symbol	Fold change (gene array)	P-value (gene array)	Fold change (RT–qPCR)	P-value (RT–qPCR)
UCP2–/– groups vs UCP2+/+ groups	PPARγ	1.91	0.0053975	2.5 ± 0.11	0.001
	Acsl3	1.6	0.0003178	1.89 ± 0.03	0.006
	Dbi	1.71	0.0137553	2.0 ± 0.27	0.002
	Lpl	1.62	0.0051632	1.94 ± 0.20	0.0001
	Me1	1.75	0.0000479	2.0 ± 0.18	0.018
	Scd1	1.88	0.0035999	2.1 ± 0.21	0.035
	Fads2	1.54	0.006165	1.68 ± 0.18	0.012
	PPARα	0.96	0.453672	0.98 ± 0.05	0.33
	PPARδ	1.01	0.903472	1.03 ± 0.09	0.86

The quantitative reverse transcription polymerase chain reaction (RT–qPCR) results were consistent with those of the gene array. UCP2, uncoupling protein 2.

the liver. The gene array and RT–qPCR showed that the expression levels of these isoforms were not significantly different between UCP2–/– group and UCP2+/+ group (Table 6). The expression of PPARγ, PPARα and PPARδ were not significantly different between the UCP2–/– group and UCP2+/+ group on the normal diet.

DISCUSSION

Hyperglycemia caused by a long-term high-fat diet could be due to insufficient insulin secretion, decreased insulin sensitivity or some combination of both[3]. In the present study, we found that blood glucose and β-cell function were better in UCP2–/– mice compared with the UCP2+/+ group on a long-term high-fat diet. Furthermore, enhanced insulin sensitivity was observed in the UCP2 –/– mice. The results were in accordance with the previous study[15]. The previous study also raised the question that although UCP2–/– mice had markedly elevated serum insulin levels, whether they could easily develop insulin resistance was still controversial. It has been reported that UCP2-deficient ob/ob mice show improved blood glucose mainly as a result of improvements in β-cell function and not enhanced insulin sensitivity[7]. These results suggest the importance of genetic background when analyzing the role of UCP2[16]. In the present study, UCP2 deficiency improved blood glucose by simultaneously promoting β-cell function and insulin sensitivity. The improved blood lipid profiles probably promoted insulin sensitivity in the UCP2–/– mice to some extent.

In our gene array research, we investigated the influence of UCP2 deficiency on the liver, the changes of related signaling pathways and gene expression. The differentially expressed genes between the UCP2–/– and UCP2+/+ group were mapped to 23 pathways. The fourth most significant pathway was the PPAR signaling pathway, which is closely related to insulin sensitivity and is involved in glucose and lipid metabolism[17,18]. PPAR agonists play an important role in the treatment of obesity-induced type 2 diabetes[19,20]. The present study used gene arrays to show that the PPAR signaling pathway is involved in the improvement of glucose and lipid metabolism in the liver tissues of UCP2-deficient mice on a long-term high-fat diet.

The liver is the organ in which expression of UCP2 is low in basal conditions, and it mainly highly expresses in Kupffer cells[21]. However, in situations of metabolic stress, like on a long-term high fat diet, UCP2 expression is induced in the liver, and enhanced expression appears mainly in hepatocytes[22]. PPARs play pivotal roles in the control of the transcription of UCP2[17,23,24]. PPARs have three isoforms, including PPARα, PPARδ and PPARγ. PPARγ is a regulator of lipid and glucose metabolism, and therefore its synthetic ligands such as glitazone – the derivatives of thiazolidinediones (e.g., troglitazone, rosiglitazone and pioglitazone) – improve insulin and glucose parameters, and increase whole body insulin sensitivity. These PPARγ synthetic ligands could indirectly increase insulin-stimulated glucose uptake in adipocytes, skeletal muscle cells and hepatocytes[17,25,26]. The present study found the UCP2-deficient mice fed a long-term high-fat diet had better insulin sensitivity, improved lipid metabolism and upregulated expression of PPARγ in the PPAR signaling pathway, which suggested the ameliorated lipid metabolism and insulin sensitivity in UCP2 deficient mice probably through PPARγ. It has been suggested that fatty acids might be key factors determining the control of UCP2 expression in the liver[27]. Excessive fatty acids intake could enhance UCP2 gene expression through PPARs[16]. In cultured hepatocytes, regulation of UCP2 gene expression is induced through PPARγ[23]. Although PPARγ is largely present in adipose tissues, and is expressed at very low levels in the liver under basal conditions, its levels are increased after consumption of a high-fat diet[23,28]. Although PPARα plays a major role in the regulation of UCP2 expression in the liver under physiological conditions, PPARγ is highly expressed in the livers of PPARα-null mice fed a high-fat diet, and it is associated with the induction of UCP2 gene expression[23]. The adenoviral-induced overexpression of PPARγ in the livers of PPARα-null mice could lead to the decreased expression of UCP2[27].

According to these previous studies on the effects of high-fat diet consumption, the expression of PPARδ also increases in the liver[29]; therefore, it has been speculated that PPARγ and PPARδ might have functions in the livers of mice fed a high-fat diet. The present study found that the expression of PPARγ significantly increased in the livers of the UCP2−/− mice fed a long-term high-fat diet, whereas the expression of PPARα and PPARδ was unaltered. Furthermore, in the UCP2+/+ groups where PPAR isoforms were unaltered, UCP2 significantly increased in the high-fat diet group. All these indicate that the deficiency of UCP2 probably has an effect on PPARγ. It was most likely that among PPAR isoforms, PPARγ was the major regulator of UCP2 in the liver under these conditions.

In summary, the present study suggested that in the mice fed a long-term high-fat diet, UCP2 deficiency led to the amelioration of lipid metabolism, and improved blood glucose by simultaneously promoting insulin sensitivity and β-cell function. The manifestation combined with the gene array assay showed that UCP2 in the liver regulates hepatic gene expression including the PPAR signaling pathway through a feedback way; in the liver, the PPAR signaling pathway played important roles in hepatic glucose and lipid metabolism in the UCP2-deficient mice. The manipulation of UCP2 protein expression could represent a new strategy for the prevention and treatment of diabetes.

ACKNOWLEDGMENTS

DISCLOSURE

The authors declare no conflict of interest.

REFERENCES

1. Polonsky KS, Sturis J, Bell GI. Non-insulin-dependent diabetes mellitus – a genetically programmed failure of the beta cell to compensate for insulin resistance. *N Engl J Med* 1996; 334: 777–783.
2. Kahn CR. Banting Lecture. Insulin action, diabetogenes, and the cause of type II diabetes. *Diabetes* 1994; 43: 1066–1084.
3. McGarry JD, Dobbins RL. Fatty acids, lipotoxicity and insulin secretion. *Diabetologia* 1999; 42: 128–138.
4. Donadelli M, Dando I, Fiorini C, *et al.* UCP2, a mitochondrial protein regulated at multiple levels. *Cell Mol Life Sci* 2014; 71: 1171–1190.
5. Fleury C, Neverova M, Collins S, *et al.* Uncoupling protein-2: a novel gene linked to obesity and hyperinsulinemia. *Nat Genet* 1997; 15: 269–272.
6. Gembal M, Detimary P, Gilon P, *et al.* Mechanisms by which glucose can control insulin release independently from its action on adenosine triphosphate-sensitive K+ channels in mouse B cells. *J Clin Invest* 1999; 91: 871–880.
7. Zhang CY, Baffy G, Perret P, *et al.* Uncoupling protein-2 negatively regulates insulin secretion and is a major link between obesity, beta cell dysfunction, and type 2 diabetes. *Cell* 2001; 105: 745–755.
8. Pi J, Collins S. Reactive oxygen species and uncoupling protein 2 in pancreatic beta-cell function. *Diabetes Obes Metab* 2010; 12: 141–148.
9. Pi J, Bai Y, Daniel KW. Persistent oxidative stress due to absence of uncoupling protein 2 associated with impaired pancreatic beta-cell function. *Endocrinology* 2009; 150: 3040–3048.
10. Diano S, Horvath TL. Mitochondrial uncoupling protein 2 (UCP2) in glucose and lipid metabolism. *Trends Mol Med* 2012; 18: 52–58.
11. Liu J, Li J, Li WJ, *et al.* The role of uncoupling proteins in diabetes mellitus. *J Diabetes Res* 2013; 2013: 585897.
12. Patanè G, Anello M, Piro S, *et al.* Role of ATP production and uncoupling protein-2 in the insulin secretory defect induced by chronic exposure to high glucose or free fatty acids and effects of peroxisome proliferator-activated receptor-gamma inhibition. *Diabetes* 2002; 51: 2749–2756.
13. Nakamura A, Tajima K, Zolzaya K, *et al.* Protection from non-alcoholic steatohepatitis and liver tumourigenesis in high fat-fed insulin receptor substrate-1-knockout mice despite insulin resistance. *Diabetologia* 2012; 55: 3382–3391.
14. Zheng J, Xiao X, Zhang Q, *et al.* Maternal high-fat diet modulates hepatic glucose, lipid profiles and gene expression in the PPAR pathway in the early life of offspring. *Int J Mol Sci* 2014; 15: 14967–14983.
15. Joseph JW, Koshkin V, Zhang CY, *et al.* Uncoupling protein 2 knockout mice have enhanced insulin secretory capacity after a high-fat diet. *Diabetes* 2002; 51: 3211–3219.
16. Toda C, Diano S. Mitochondrial UCP2 in the central regulation of metabolism. *Best Pract Res Clin Endocrinol Metab* 2014; 28: 757–764.
17. Ferré P. The biology of peroxisome proliferator-activated receptors: relationship with lipid metabolism and insulin sensitivity. *Diabetes* 2004; 53(Suppl 1): S43–S50.
18. Mansour M. The roles of peroxisome proliferator-activated receptors in the metabolic syndrome. *Prog Mol Biol Transl Sci* 2014; 121: 217–266.
19. Kliewer SA, Xu HE, Lambert MH. Peroxisome proliferator-activated receptors: from genes to physiology. *Recent Prog Horm Res* 2001; 56: 239–263.
20. Pershadsingh HA. Dual peroxisome proliferator-activated receptor- α/γ agonists: in the treatment of type 2 diabetes mellitus and the metabolic syndrome. *Treat Endocrinol* 2006; 5: 89–99.
21. Larrouy D, Laharrague P, Carrera G, *et al.* Kupffer cells are adominant site of uncoupling protein 2 expression in rat liver. *Biochem Biophys Res Commun* 1997; 235: 760–764.

22. Nakatani T, Tsuboyama-Kasaoka N, Takahashi M, et al. Mechanism for peroxisome proliferator-activated receptor-α activator-induced up-regulation of UCP2 mRNA in rodent hepatocytes. J Biol Chem 2002; 277: 9562–9569.

23. Villarroya F, Iglesias R, Giralt M. PPARs in the control of uncoupling proteins gene expression. PPAR Res 2007; 2007: 74364.

24. Bugge A, Siersbaek M, Madsen MS, et al. A novel intronic peroxisome proliferator-activated receptor gamma enhancer in the uncoupling protein (UCP) 3 gene as a regulator of both UCP2 and -3 expression in adipocytes. J Biol Chem 2010; 285: 17310–17317.

25. Tan MH. Current treatment of insulin resistance in type 2 diabetes mellitus. Int J Clin Pract Suppl 2000; 113: 54–62.

26. Deeg MA, Tan MH. PPAR Res 2008; 2008: 520465.

27. Memon RA, Tecott LH, Nonogaki K. Upregulation of peroxisome proliferator-activated receptor (PPAR-α) and PPAR-γ messenger ribonucleicacid expression in the liver in murine obesity: troglitazone induces expression of PPAR-α-responsive adipose tissue-specific genes in the liver of obese diabetic mice. Endocrinology 2000; 141: 4021–4031.

28. Bojic LA, Telford DE, Fullerton MD, et al. PPARδ activation attenuates hepatic steatosis in Ldlr−/− mice by enhanced fat oxidation, reduced lipogenesis, and improved insulin sensitivity. J Lipid Res 2014; 55: 1254–1266.

29. Wright MB, Bortolini M, Tadayyon M, et al. Minireview: challenges and opportunities in development of PPAR agonists. Mol Endocrinol 2014; 28: 1756–1768.